Low-Friction Nanoscale Linear Bearing Realized from Multiwall Carbon Nanotubes

John Cumings and A. Zettl*

We demonstrate the controlled and reversible telescopic extension of multiwall carbon nanotubes, thus realizing ultralow-friction nanoscale linear bearings and constant-force nanosprings. Measurements performed in situ on individual custom-engineered nanotubes inside a high-resolution transmission electron microscope demonstrated the anticipated van der Waals energy–based retraction force and enabled us to place quantitative limits on the static and dynamic interwall frictional forces between nested nanotubes. Repeated extension and retraction of telescoping nanotube segments revealed no wear or fatigue on the atomic scale. Hence, these nanotubes may constitute near perfect, wear-free surfaces.

Multiwall carbon nanotubes (MWNTs) comprise concentric cylindrical layers or shells of graphite-like sp^2-bonded carbon, where the intershell interaction is predominantly van der Waals (*1*). In analogy to the well-known lubricating properties of van der Waals–bonded graphite, the individual cylinders of MWNTs might be expected to easily slide or rotate with respect to one another, forming near ideal linear and rotational nanobearings. Recent theoretical calculations (*2, 3*) indicate that the MWNT interlayer corrugation energy is indeed small and would favor such motion. For a MWNT, one could envision an extension mode much like the "telescoping" of a mariner's traditional spyglass. Some evidence for inadvertent MWNT telescopic extension can be found in severe mechanical stress failure mode studies, including studies of MWNTs embedded in a stressed polymer composite (*4*) and MWNTs torn apart in quasi-static tensile stress measurements performed in a scanning electron microscope (*5*). However, no controlled and reversible telescoping of MWNTs has been previously achieved.

A major difficulty in initiating controlled telescoping in MWNTs is the commonly capped ends, which seal in all inner-core nanotube cylinders. Even if the MWNT ends are opened by methods such as acid etching, it is difficult to selectively contact just the core tubes. Recently, a method (*6*) was discovered whereby the ends of a MWNT can be carefully opened. The procedure removes the caps from just the outer-shell nanotubes while leaving the core nanotubes fully intact and protruding. We have used this technique inside a high-resolution transmission electron microscope (TEM) to attach a movable nanomanipulator (*7*) to only the core nanotubes within a MWNT. In situ manipulation of the nanotube core allows controlled reversible telescoping to be achieved and the associated forces to be quantified. Robust ultralow-friction linear nanobearings and (constant-force) nanosprings are demonstrated.

The configurations used inside the TEM (Topcon 002b operating at 100 kV) for the different mechanical experiments are shown schematically in Fig. 1. First, a fiber rich in MWNTs produced by conventional arc-plasma methods is rigidly mounted using silver cement to a stationary gold electrode. The free end of an individual MWNT (Fig. 1A) is then engineered (*6*) to expose the core tubes (Fig. 1B). In Fig. 1C, the nanomanipulator is brought into contact with the core tubes and is spot-welded to the core by means of a short, controlled electrical current pulse; this is the common starting point for the two classes of experiments depicted in Fig. 1, D and E. In Fig. 1D, the manipulator is moved right and left, thus telescoping the core out from or reinserting it into the outer housing of nanotube shells. The extraction and reinsertion process can be repeated many times while viewing the MWNT at high TEM resolution to test for atomic-scale nanotube surface wear and fatigue. In Fig. 1E, the manipulator first telescopes the inner core out, then fully disengages, which allows the core to be drawn back into the outer shells by the intertube van der Waals force, consequently lowering the total system energy. A real-time video recording of the core bundle dynamics gives information pertaining to van der Waals and frictional forces.

A TEM image of a MWNT in a fully telescoped position is shown in Fig. 2. Using higher resolution imaging than that used for Fig. 2, we determined that this MWNT originally had nine walls, with an outer diameter of 8 nm and an inner diameter of 1.3 nm. After extension, a core segment 4 nm in diameter (consisting of four concentric walls) has been almost completely extracted from the outer-shell structure. The telescoping process was found to be fully reversible, in that the core could be completely pushed back into the outer shells, restoring the MWNT to its original "retracted" condition. The process of extending and retracting the core was repeated about 20 times for several different MWNTs, and in all cases no apparent damage to the "sliding" surfaces—that is, the outer tube of the core or the inner tube of the shell structure—was observed, even under the highest TEM resolution conditions (~2 Å). The apparent lack of induced defects or other structural changes in the nanotube contact surfaces at the atomic level suggests strongly that these near atomically perfect nanotube structures may be wear-free and will not fatigue even after a very large number of cycles.

In the engineering of macroscopic bearings, the moving parts are typically cycled 10^3 to 10^9 times before definitive conclusions about wear can be drawn, because the damage from a single cycle is microscopic and cannot be readily observed by eye or even by conventional microscopy. In this case, we are examining bearings at the atomic scale, and we find that after each cycle the atomic structure of the

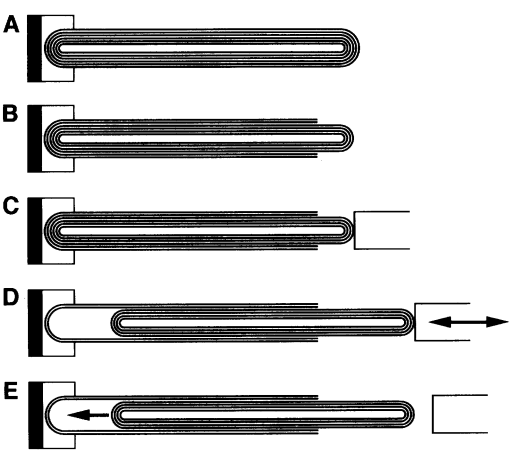

Fig. 1. Schematic representation of the experiments performed inside the TEM. (**A** to **C**) The process of opening the end of a MWNT (A), exposing the core tubes (B), and attaching the nanomanipulator to the core tubes (C). (**D** and **E**) Two different classes of subsequent experiments performed. In (D), the nanotube is repeatedly telescoped while observations for wear are performed. In (E), the core is released and pulled into the outer-shell housing by the attractive van der Waals force.

Department of Physics, University of California, Berkeley, CA 94720, USA, and Materials Sciences Division, Lawrence Berkeley National Laboratory, Berkeley, CA 94720, USA.

*To whom correspondence should be addressed. E-mail: azettl@physics.berkeley.edu

nanotubes is unaffected by the motion. Hence, we conclude that the nanotube sections are near perfect sliding surfaces, apparently free from wear for all cycles.

In all MWNTs that we have examined, all repeated sliding motion for a given MWNT was observed to take place between the same two nanotube shells; similarly, no "multiple" telescoping was observed (where the total length of the nanotube might become more than double the length of the original MWNT, as would occur from "sticking" of the segments at some point in their extension). We interpret this repeatability as a self-selection process where the most perfect surfaces offer the least resistance to motion. Even after repeated motions, the same surfaces remained the "most favored" ones, again providing evidence for no sliding-induced wear on the active surfaces. In a many-walled MWNT, even the catastrophic failure, such as fusing, of one surface pair would not render the MWNT bearing unusable, as another (nearly equally perfect) surface pair would then become the active elements.

In some cases, a small amount of residual amorphous carbon was produced during the initial core exposure process. However, because of the extremely small interwall clearance in MWNTs, such contamination appears to have no effect on the bearing action, as it is simply brushed away upon reinsertion of the core section into the nanotube housing. Hence, MWNT-based linear bearings are self-cleaning and immune from typical contaminant-induced wear.

Several internal forces are associated with telescoping MWNTs. To first order, these consist of the van der Waals–derived force and possible static and dynamic frictional forces. The van der Waals force is given by

$$F_{vdW} = -\frac{d}{dx}U(x) \qquad (1)$$

where the van der Waals energy (*8*) is given by $U(x) = -0.16Cx$ (expressed in joules), where C is the circumference of the "active" nanotube bearing cylinders and x is the length of the overlap between the core section and the outer walls (expressed in meters). The lowering in van der Waals energy that results from increasing the tube-tube contact area tends to retract the extended core of a telescoped MWNT. Interestingly, because the active intertube contact area decreases linearly with core tube extension, this restoring force is independent of contact area, or equivalently, independent of core extension. Hence, a telescoped nanotube with only one active (sliding) surface pair is expected to act as a constant-force spring.

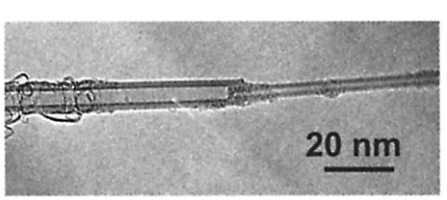

Fig. 2. A TEM image of a telescoped nanotube. This particular nanotube originally had nine shells, but upon telescoping a four-shell core has been nearly completely extracted.

To determine experimentally whether F_{vdW} dominates nanotube linear bearing dynamics, we used the configuration described in Fig. 1E. The core tubes of a MWNT were first telescoped using the carbon-tipped manipulator and then released. Little is known about the exact nature of the spot-weld junction, but presumably it represents carbon-carbon bonds similar to those of polymerized fullerenes. Lateral deflections of the manipulator were used to fatigue and eventually break the spot weld, thus releasing the core segment. The resulting accelerated motion of the released core segment was recorded using a continuous video system tied to the TEM imaging electronics.

Several selected frames from one such video recording are shown in Fig. 3. The upper five frames show the core segment being slowly and successively telescoped to the right (the structure in the left third of the image seen crossing the MWNT at about a 30° angle is another nanotube unrelated to the experiment, and it is not in physical contact with the subject MWNT). Just after the fifth frame, the manipulator has released the core segment. The sixth and final frame, which occurred one video frame after the release of the nanotube, shows the core after it rapidly and fully retracted inside the outer shells of the MWNT. The dimensions for the core segment of the MWNT in Fig. 3 yield a core segment mass of 2.9×10^{-16} g. Combining this with $C = 57$ nm and the initial extension of 330 nm, Eq. 1 leads to complete retraction of the core tubes in 4.6 ns. This derived value is consistent with our experimental observation that the complete contraction occurred in less than one video frame (33 ms).

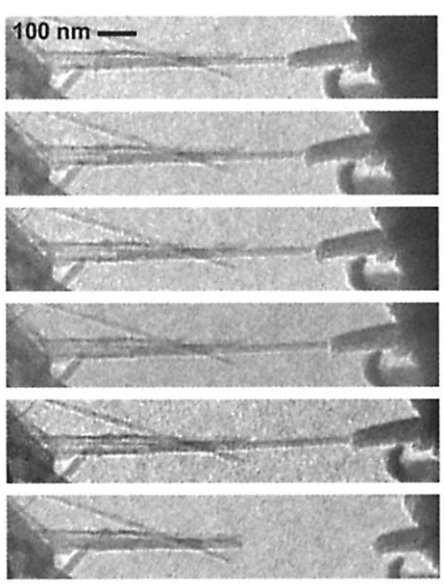

Fig. 3. Selected frames of a video recording of the in situ telescoping of a MWNT. In the first five frames, the core nanotubes are slowly withdrawn to the right. In the sixth image, which occurred one video frame after the core was released, the core has fully retracted into the outer nanotube housing as a result of the attractive van der Waals force.

From our observations, we can also draw conclusions about the static and dynamic friction between concentric shells of a multiwall nanotube. Although macroscopic models of friction between solids dictate that friction is proportional to normal force, independent of contact area, modern microscopic models of friction predict that friction is in fact proportional to contact area (*9*). In macroscopically rough samples, the actual contact occurs at point asperities, and the microscopic contact area is proportional to the total normal force. Nanotube shells, however, are atomically smooth, so any interlocking between the shells (due, for example, to the atomic corrugations) is best estimated by using the entire surface area of contact. The F_{vdW} retraction force for the nanotube in Fig. 3 is calculated to be only 9 nN. This value suggests that the static friction force $f_s < 2.3 \times 10^{-14}$ N per atom (6.6×10^{-15} N/Å^2). Furthermore, because the tube contracts fully, we conclude that the dynamic friction force $f_k < 1.5 \times 10^{-14}$ N per atom ($4.3 \times$

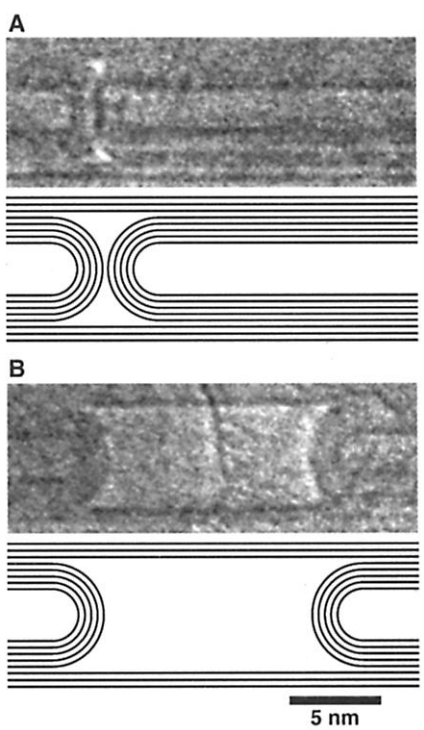

Fig. 4. TEM images of a bamboo section of a MWNT. (**A**) An as-grown bamboo section. (**B**) The same area after the core tubes on the right have been telescoped outward. Bamboo sections are independent and are free to slide inside their nanotube housing. The line drawings beneath the images are schematic representations to guide the eye.

10^{-15} N/Å^2). Friction is an important concern in small-scale systems such as microelectromechanical systems (MEMS) (*10*), and recent atomic-scale frictional force measurements (*11, 12*) using conventional materials yield values about three orders of magnitude greater than the upper-limit frictional forces found here for MWNT surfaces.

If the (already generally small) friction between nanotube shells is indeed proportional to the length of the overlapping sections, then minimum bearing friction would be obtained for the shortest possible nanotube core-housing overlap. Several possibilities exist to achieve this configuration. First, a very short MWNT might be used from the outset. Second, the core of a long MWNT could be telescoped nearly all the way out, yielding a short contact area. The third possibility takes advantage of "bamboo" configurations (*13*) that sometimes occur in MWNTs, where the inner nanotube sections do not extend along the entire length of the MWNT, but rather represent an end-to-end series of shorter, fully capped, nanotube segments residing inside the continuous housing of outer nanotube shells. A TEM image of such a bamboo joint inside a larger MWNT is shown in Fig. 4A. In Fig. 4B, the core segment on the right has been telescoped out, cleanly separating the bamboo joint. This result shows that bamboo nanotube core segments are truly independent sections with weak end-to-end binding. This observation has important practical implications for common-axis bearings: Short independent bamboo sections might serve as ultralow-friction linear or rotational bearings that are firmly embedded in a common long, stiff cylindrical housing.

Our results demonstrate that MWNTs hold great promise for nanomechanical or nanoelectromechanical systems (NEMS) applications. Low-friction, low-wear nanobearings and nanosprings are essential ingredients in general NEMS technologies. The transit time for complete nanotube core retraction (on the order of 1 to 10 ns) implies the possibility of exceptionally fast electromechanical switches.

References and Notes

1. S. Iijima, *Nature* **354**, 56 (1991).
2. A. Kolmogorov and V. Crespi, *Bull. Am. Phys. Soc.* **45**, 254 (2000).
3. V. H. Crespi, P. Zhang, P. E. Lammert, in *Electronic Properties of Novel Materials—Science and Technology of Molecular Nanostructures*, H. Kuzmany, J. Fink, M. Mehring, S. Roth, Eds. (American Institute of Physics, College Park, MD, 1999), pp. 364–368.
4. H. D. Wagner, O. Lourie, Y. Feldman, R. Tenne, *Appl. Phys. Lett.* **72**, 188 (1998).
5. M. F. Yu *et al.*, *Science* **287**, 637 (2000).
6. J. Cumings, P. G. Collins, A. Zettl, *Nature*, in press.
7. P. Poncharal, Z. L. Wang, D. Ugarte, W. A. De Heer, *Science* **283**, 1513 (1999).
8. L. X. Benedict *et al.*, *Chem. Phys. Lett.* **286**, 490 (1998).
9. B. N. J. Persson, *Surf. Sci. Rep.* **33**, 83 (1999).
10. W. Trimmer, *Micromechanics and MEMS: Classic and Seminal Papers to 1990* (IEEE Press, New York, 1997).
11. R. W. Carpick, D. F. Ogletree, M. Salmeron, *Appl. Phys. Lett.* **70**, 1548 (1997).
12. M. Enachescu *et al.*, *Phys. Rev. Lett.* **81**, 1877 (1998).
13. S. Iijima, P. M. Ajayan, T. Ichihashi, *Phys. Rev. Lett.* **69**, 3100 (1992).

14. We thank U. Dahmen, C. Nelson, E. Stach, M. L. Cohen, and S. G. Louie for helpful interactions. Supported by the Office of Energy Research, Office of Basic Energy Sciences, Division of Materials Sciences, U.S. Department of Energy (contract DE-AC03-76SF00098) and by NSF grants DMR-9801738 and DMR-9501156.

9 March 2000; accepted 21 June 2000

Full Three-Dimensional Photonic Bandgap Crystals at Near-Infrared Wavelengths

Susumu Noda,[1]* Katsuhiro Tomoda,[1] Noritsugu Yamamoto,[2] Alongkarn Chutinan[1]

An artificial crystal structure has been fabricated exhibiting a full three-dimensional photonic bandgap effect at optical communication wavelengths. The photonic crystal was constructed by stacking 0.7-micrometer period semiconductor stripes with the accuracy of 30 nanometers by advanced wafer-fusion technique. A bandgap effect of more than 40 decibels (which corresponds to 99.99% reflection) was successfully achieved. The result encourages us to create an ultra-small optical integrated circuit including a three-dimensional photonic crystal waveguide with a sharp bend.

There is much interest in photonic crystals (*1–3*) in which the refractive index changes periodically. A photonic bandgap is formed in the crystals, and the propagation of electromagnetic waves is prohibited for all wave vectors. Various scientific and engineering applications, such as control of spontaneous emission, zero-threshold lasing, sharp bending of light (*4*), and so on, are expected by using the photonic bandgap and the artificially introduced defect states and/or light-emitters. To realize the potential of photonic crystals as much as possible, the following requirements should be satisfied: (i) construction of a three-dimensional (3D) photonic crystal with a complete photonic bandgap in the optical wavelength region, (ii) introduction of an arbitrary defect state into the crystal at an arbitrary position, (iii) introduction of an efficient light-emitting element, and (iv) use of an electronically conductive crystal, which is desirable for the actual device application. Although various important approaches such as a self-assembled colloidal crystal (*5*), a GaAs-based three-axis dry-etching crystal (*6*), and a silicon-based layer-by-layer crystal (*7, 8*) with a so-called woodpile structure (*9*) have been proposed and investigated to construct the 3D photonic crystals, it is considered difficult for these methods to satisfy the four above requirements simultaneously.

[1]Department of Electronic Science and Engineering, Kyoto University, Yoshida-honmachi, Sakyo-ku, Kyoto 606-8501, Japan. [2]Electrotechnical Laboratory, Agency of Industrial Science and Technology (AIST), Ministry of International Trade and Industry (MITI), 1-1-4, Umezono, Tsukuba, Ibaraki, 305-8568, Japan.

*To whom correspondence should be addressed. E-mail: snoda@kuee.kyoto-u.ac.jp

Recently, we reported a complete 3D photonic crystal at infrared (5 to 10 μm) (*10–12*) to near-infrared wavelengths (1 to 2 μm) (*12*) based on a method in which III-V semiconductor stripes are stacked with the wafer-fusion and laser beam–assisted very precise alignment techniques to construct the woodpile structure. Because the crystal is constructed with III-V semiconductors, which are widely used for optoelectronic devices, the above requirement (iii) is satisfied. Moreover, as the wafer-fusion technique enables us to construct an arbitrary structure and to form an electronically active interface, all requirements (i) through (iv) will be satisfied.

However, an important issue remains to be solved: the photonic crystal with sufficient bandgap effects has not yet been realized at near-infrared wavelengths. The bandgap effect at near-infrared wavelengths was much weaker (by more than a factor of 10) than those at infrared wavelengths. A very weak effect was observed also in silicon-based layer-by-layer crystals (*8*). This is certainly due to the structural fluctuations caused by the imperfection of material process when the size is in the submicrometer range, which leads to serious problems for the actual scientific applications such as complete control of spontaneous emission and very sharp bending of light. We developed the advanced processing technique to address the above issue and to fabricate 3D photonic crystals with sufficient bandgap effects at near-infrared wavelengths. It is also shown that the crystal is applicable to ultra-small optical integrated circuits, including a 3D waveguide with a sharp bend.

In the crystal structure studied here (Fig. 1A), where one unit of woodpile structure is